INTERNATIONAL JOURNAL FOR NUMERICAL METHODS IN FLUIDS
Int. J. Numer. Meth. Fluids **28**: 1265–1280 (1998)

STUDY OF THE EFFECT OF THE NON-ORTHOGONALITY FOR NON-STAGGERED GRIDS—THE THEORY

H. XU* AND C. ZHANG

Department of Mechanical and Materials Engineering, University of Windsor, Windsor, Ontario N9B 3P4, Canada

SUMMARY

An investigation has been conducted to determine the effect of the grid non-orthogonality on the convergence behavior of two-dimensional lid-driven cavity flows. The relevant theory is presented in this article. In the present work, the contravariant velocity fluxes are used as the dependent variables on non-orthogonal, non-staggered grids. The momentum equations retain a strongly conservative form. Two practices for treating the momentum interpolation method in general curvilinear co-ordinates are presented. In each practice, the momentum interpolation formulations with and without velocity underrelaxation factor are considered. The discretization equations are solved using the SIMPLE, SIMPLEC and SIMPLER algorithms. © 1998 John Wiley & Sons, Ltd.

KEY WORDS: momentum interpolation; contravariant velocity fluxes; general curvilinear co-ordinates; non-staggered grid; lid-driven cavity flow

1. INTRODUCTION

Most practical fluid flows occur in complex geometrical configurations. Examples can be found in such diverse areas as aerodynamics, meteorology, nuclear reactor design, turbomachinery and physiology. Although the finite element method appears to be a natural choice due to its intrinsic geometrical flexibility, the discretized equations for this method are difficult to derive. The finite difference (volume) method is more likely to be used for the numerical simulation of fluid flows because its implementation, compared with that of the finite element method, is very easy and straightforward. However, the application of this method has certain difficulties and uncertainties in the complex geometries. The major shortcoming is that this method requires the boundaries of the physical domain to be regular and to coincide with the co-ordinate system. Otherwise, an elaborate treatment of the boundaries must be made, namely, an interpolation must be used in the application of the boundary conditions for the irregular shapes and sizes of boundary cells. An alternative is to generate an orthogonal mesh which fits the boundaries. However, an apparent shortcoming is that the co-ordinate lines of curvilinear orthogonal co-ordinates are normal to each other. This feature limits its use in most practical fluid flows where irregular boundaries prevail. This difficulty can be overcome by using a non-orthogonal mesh. When applying this method, a body-fitted co-ordinate system is

* Correspondence to: Department of Mechanical and Materials Engineering, University of Windsor, Windsor, Ontario N9B 3P4, Canada.

CCC 0271–2091/98/191265–16$17.50

Received February 1997
Revised May 1997

defined as a general curvilinear co-ordinate system which follows the boundaries of an irregular flow field. When partial differential equations are transformed onto such a co-ordinate system, finite difference representations can be made using only the neighboring grid nodes regardless of the boundary shape or even its movement. The grid lines can be distributed by a grid generator [1] and mapped from the physical space to the computational space. Thus, all the computations can be carried out on a fixed rectangular grid in the computational domain.

The difference among various numerical methods using non-orthogonal grids lies in two aspects. One is the selection of the dependent variables in the momentum equations. Another is the grid arrangement. The dependent variables in the momentum equations in general curvilinear co-ordinates can be Cartesian velocity components or non-Cartesian velocity components. The latter include contravariant components and covariant components, physical contravariant components and physical covariant components, contravariant projections (resolutes) and covariant projections.

Mathematically, governing equations in general curvilinear co-ordinates are obtained by employing two different approaches. One is the 'partial transformation'. Another is the 'complete transformation'. Normally, the partial transformation leads to a strongly conservative form of the Navier–Stokes equations in general curvilinear co-ordinates. The Cartesian velocity components are usually used as the dependent variables. The complete transformation leads to a weakly conservative form of the Navier–Stokes equations. The non-Cartesian velocity components are usually used as the dependent variables. Karki [2] proposed a calculation procedure in which the complete transformation is avoided but the strongly conservative form of the Navier–Stokes equations in which the non-Cartesian velocity components can be used as the dependent variables is still retained. Yang *et al.* [3] improved this technique, in which the differentiation operators are applied directly to the velocity vector itself instead of velocity components. This can eliminate the numerical diffusion due to the skewness of a flow relative to grid lines.

Another consideration in the numerical simulations is the grid arrangement. To avoid the splitting of the pressure field which satisfies the momentum equations but is physically unrealistic, a common practice is to use a staggered grid arrangement. In this arrangement, the scalar quantities such as pressure are stored at the main grid nodes, whereas the velocity components, whether Cartesian or non-Cartesian components, are stored at the faces or the corners of the control volumes. A full description regarding the staggered grid arrangement can be found in Reference [2]. Although it can successfully prevent the oscillating pressure field, a staggered grid arrangement also has its own disadvantages. One of the disadvantages is that the calculations of the coefficients and the geometrical interpolation factors are more time-consuming when different control volumes are used for different variables. Also, more interpolations which are necessary for the evaluation of the flow rate at the cell faces may lead to higher numerical inaccuracy. A non-staggered grid arrangement, due to its geometrical simplicity, is very attractive. In this arrangement, the scalar quantities and the velocity components are all stored at the same grid nodes. However, the linear interpolations used to express the gradients of the pressure in the momentum equations and the velocity variation in the continuity equation usually result in non-physical oscillation if a non-staggered grid is used. Special measures must be taken to prevent the splitting of the pressure field. Rhie and Chow [4] made the first successful attempt to prevent the pressure oscillation on non-staggered grids in two-dimensional curvilinear co-ordinates. They employed an interpolation practice called momentum interpolation to evaluate the cell-face velocities. The key idea is to calculate the cell-face velocities using the discretized momentum equations for two adjacent grid nodes

separated by the face. Majumdar [5] presented more general formulations of the momentum interpolation in Cartesian co-ordinates in which the velocity underrelaxation factor appears. He found that whether a unique converged solution for a flow field can be obtained depends on the velocity underrelaxation factor used in the momentum interpolation formulations. He proposed an iterative algorithm to employ the momentum interpolation formulation in order to achieve a unique solution that is independent of the velocity underrelaxation factor. Miller and Schmidt [6] developed a momentum interpolation. They estimated the degree of the dependence of numerical solutions on the velocity underrelaxation factor and obtained a formulation of the momentum interpolation which is independent of the velocity underrelaxation factor for a converged solution in Cartesian co-ordinates. The momentum interpolation method has achieved great success and is now being widely used in a variety of fluid flow calculations [7–9].

2. OBJECTIVES

Recently, the strongly conservative form of the Navier–Stokes equations in general curvilinear co-ordinates has been getting more and more attention. Relatively, the main trend has been to use the covariant velocity projections rather than the contravariant velocity components or its variant contravariant velocity fluxes [1,7–9]. The reason lies in two aspects. One is that the covariant velocity projections align with the curvilinear co-ordinates. Another, the more important reason, is that the cross pressure gradient terms in the momentum equations disappear. The merit of single pressure gradient terms in the momentum equations is that fewer interpolations are required to calculate the pressure gradients when a staggered grid arrangement is employed. However, this merit becomes unimportant if a non-staggered grid arrangement is used. If SIMPLE series algorithms are used to solve the governing equations, non-orthogonal terms in the pressure correction equation cannot be eliminated no matter what kind of the velocity components are used as the dependent variables. On the other hand, the discretized continuity equation becomes simple if the contravariant velocity components or fluxes are used as the dependent variables, although the cross pressure gradient terms in the momentum equations exist. In general curvilinear co-ordinates, the values of the contravariant velocity fluxes at the cell faces need to be evaluated to determine the coefficients (A_E, A_W, A_N, A_S, A_T, A_B) in the discretized momentum equations. A further advantage of using the contravariant velocity components or fluxes as the dependent variables is that the momentum interpolation is easily implemented and no additional calculation is needed to obtain the flow rate through the cell faces. In particular, it is convenient to change the formulation of the momentum interpolation in the computer code. In fact, Rhie and Chow [4] employed their original version of the momentum interpolation to calculate the contravariant velocity fluxes at the cell faces instead of the Cartesian velocity components, although they chose Cartesian velocity components as the dependent variables.

The purpose of the present work is to study the effect of the grid non-orthogonality on the convergence behavior. The two-dimensional lid-driven cavity flows are selected for the study. This problem has been studied by Peric [10] and Cho and Chung [11]. Their work will be described in a companion article [12]. In the present study, contravariant velocity fluxes are chosen as the dependent variables together with non-staggered grids. Different formulations of the momentum interpolation are derived based on Rhie and Chow's original version and employed to test their abilities to give a converged solution on non-orthogonal grids. The SIMPLE [13], SIMPLEC [14] and SIMPLER [15] algorithms are used to solve the discretiza-

tion equations respectively. It can be expected that combinations of different formulations of the momentum interpolation with different algorithms (SIMPLE, SIMPLEC, SIMPLER) will demonstrate different convergence behaviors. The relevant theory is presented in this article. Results will be given and discussed in a companion article [12].

3. CONSERVATION EQUATIONS

The steady state governing equations for a general dependent variable ϕ can be written in the following compact form

$$\nabla \cdot \boldsymbol{J} = S^{\phi}, \tag{1}$$

where S^{ϕ} denotes the source term and $\boldsymbol{J}$ is the total flux made up of the convection flux and the diffusion flux. $\boldsymbol{J}$ is given by

$$\boldsymbol{J} = \rho \boldsymbol{u} \phi - \Gamma \nabla \phi, \tag{2}$$

where ρ is the density of the fluid and Γ is the diffusivity. For momentum equations, Γ is the dynamic viscosity. In Cartesian co-ordinates, $\boldsymbol{J}$ can be expressed as

$$\boldsymbol{J} = J^{x^i} \boldsymbol{i}_i, \tag{3}$$

where x^i denotes the Cartesian co-ordinates and $\boldsymbol{i}_i$ is the unit vector. J^{x^i} is the Cartesian components of $\boldsymbol{J}$ and is given by

$$J^{x^i} = \rho u_i \phi - \Gamma \frac{\partial \phi}{\partial x^i}, \tag{4}$$

where u_i is the Cartesian velocity component. In general curvilinear co-ordinates, $\boldsymbol{J}$ can be expressed as

$$\boldsymbol{J} = J^{\xi^j} \boldsymbol{e}_j, \tag{5}$$

where ξ^j denotes the curvilinear co-ordinates and $\boldsymbol{e}_j$ is the covariant base vector. According to tensor analysis, the following relationship between J^{ξ^j} and J^{x^i} can be obtained

$$J^{\xi^j} = \frac{\partial \xi^j}{\partial x^i} J^{x^i}. \tag{6}$$

Substituting Equation (4) into (6) leads to

$$J^{\xi^j} = \frac{\partial \xi^j}{\partial x^i} \left(\rho u_i \phi - \Gamma \frac{\partial \phi}{\partial x^i} \right). \tag{7}$$

Using the chain rule, $\partial \phi / \partial x^i$ can be written as

$$\frac{\partial \phi}{\partial x^i} = \frac{\partial \xi^k}{\partial x^i} \frac{\partial \phi}{\partial \xi^k}. \tag{8}$$

Substituting Equation (8) into (7) gives

$$J^{\xi^j} = \frac{\partial \xi^j}{\partial x^i} \left(\rho u_i \phi - \Gamma \frac{\partial \xi^k}{\partial x^i} \frac{\partial \phi}{\partial \xi^k} \right). \tag{9}$$

The divergence of $\boldsymbol{J}$ in general curvilinear co-ordinates is expressed as

$$\nabla \cdot \boldsymbol{J} = \frac{1}{Ja}\left[\frac{\partial (JaJ^{\xi^j})}{\partial \xi^j}\right], \tag{10}$$

where Ja is the Jacobian of the transformation and is expressed as

$$Ja = \begin{vmatrix} \dfrac{\partial x^1}{\partial \xi^1} & \dfrac{\partial x^1}{\partial \xi^2} & \dfrac{\partial x^1}{\partial \xi^3} \\ \dfrac{\partial x^2}{\partial \xi^1} & \dfrac{\partial x^2}{\partial \xi^2} & \dfrac{\partial x^2}{\partial \xi^3} \\ \dfrac{\partial x^3}{\partial \xi^1} & \dfrac{\partial x^3}{\partial \xi^2} & \dfrac{\partial x^3}{\partial \xi^3} \end{vmatrix} . \tag{11}$$

Using Equations (9) and (10), Equation (1) can be written as

$$\frac{1}{Ja}\frac{\partial\left[Ja\dfrac{\partial \xi^j}{\partial x^i}\left(\rho u_i \phi - \Gamma \dfrac{\partial \xi^k}{\partial x^i}\dfrac{\partial \phi}{\partial \xi^k}\right)\right]}{\partial \xi^j} = S^{\phi}. \tag{12}$$

For convenience, let

$$\bar{J}_i^j = Ja\frac{\partial \xi^j}{\partial x^i}. \tag{13}$$

Equation (12) now becomes

$$\frac{\partial\left(\bar{J}_i^j \rho u_i \phi - \dfrac{\Gamma}{Ja}\bar{J}_i^j \bar{J}_i^k \dfrac{\partial \phi}{\partial \xi^k}\right)}{\partial \xi^j} = JaS^{\phi}. \tag{14}$$

Equation (14) is the steady state governing equation for a general dependent variable ϕ in general curvilinear co-ordinates.

The contravariant velocity flux U^i is defined as

$$U^i = \bar{J}_i^j \rho u_j. \tag{15}$$

U^i is a variant of the contravariant velocity components V^i which, according to tensor analysis, can be expressed in terms of u_i as

$$V^i = \frac{\partial \xi^i}{\partial x^j}u_j = \frac{\bar{J}_j^i}{Ja}u_j. \tag{16}$$

In the present, U^i is chosen as the dependent variable. Equation (14) can be expressed as

$$\frac{\partial\left(U^j \phi - \dfrac{\Gamma}{Ja}\bar{J}_i^j \bar{J}_i^k \dfrac{\partial \phi}{\partial \xi^k}\right)}{\partial \xi^j} = JaS^{\phi}. \tag{17}$$

4. DISCRETIZATION OF THE CONSERVATION EQUATIONS

The discretization of the conservation equations is performed using the finite volume approach in the computational space. The physical space is divided into a set of hexahedrons. The grids are mapped from the physical space to the computational space using a grid generator [1].

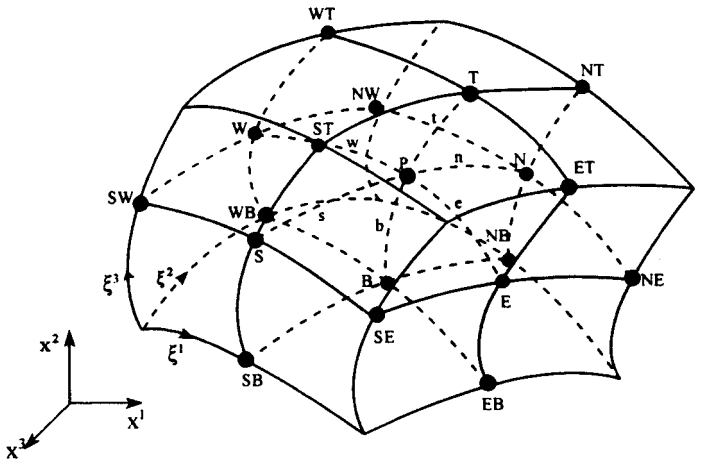

Figure 1. The grid arrangement in the physical space.

Figure 1 and Figure 2 show the grid arrangement in the physical space and the computational space, respectively. A non-staggered grid arrangement is used.

Equation (14) can be integrated over each control volume in the computational space as follows

$$\left[\left(U^1\phi - \frac{\bar{J}_k^1\bar{J}_k^1\Gamma}{Ja}\frac{\partial\phi}{\partial\xi^1}\right)\Delta\xi^2\Delta\xi^3\right]_{\mathrm{w}}^{\mathrm{e}} + \left[\left(U^2\phi - \frac{\bar{J}_k^2\bar{J}_k^2\Gamma}{Ja}\frac{\partial\phi}{\partial\xi^2}\right)\Delta\xi^1\Delta\xi^3\right]_{\mathrm{s}}^{\mathrm{n}} + \left[\left(U^3\phi - \frac{\bar{J}_k^3\bar{J}_k^3\Gamma}{Ja}\frac{\partial\phi}{\partial\xi^3}\right)\Delta\xi^1\Delta\xi^2\right]_{\mathrm{b}}^{\mathrm{t}}$$

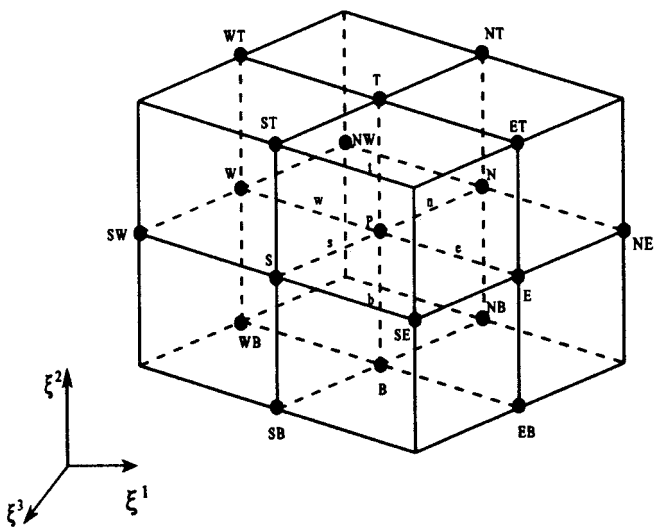

Figure 2. The grid arrangement in the computational space.

$$= \left[\frac{\Gamma}{Ja}\left(\bar{J}_k^2\bar{J}_k^1\frac{\partial\phi}{\partial\xi^2}+\bar{J}_k^3\bar{J}_k^1\frac{\partial\phi}{\partial\xi^3}\right)\Delta\xi^2\Delta\xi^3\right]_{\mathrm{w}}^{\mathrm{e}}+\left[\frac{\Gamma}{Ja}\left(\bar{J}_k^1\bar{J}_k^2\frac{\partial\phi}{\partial\xi^1}+\bar{J}_k^3\bar{J}_k^2\frac{\partial\phi}{\partial\xi^3}\right)\Delta\xi^1\Delta\xi^3\right]_{\mathrm{s}}^{\mathrm{n}}$$
$$+\left[\frac{\Gamma}{Ja}\left(\bar{J}_k^1\bar{J}_k^3\frac{\partial\phi}{\partial\xi^1}+\bar{J}_k^2\bar{J}_k^3\frac{\partial\phi}{\partial\xi^2}\right)\Delta\xi^1\Delta\xi^2\right]_{\mathrm{b}}^{\mathrm{t}}+JaS^{\phi}\Delta\xi^1\Delta\xi^2\Delta\xi^3, \tag{18}$$

where the subscripts e, w, n, s, t and b denote the cell faces on the east, west, north, south, top and bottom. In general curvilinear co-ordinates, the diffusive flux consists of the orthogonal part and the non-orthogonal part. In the present study, the convection and the orthogonal diffusion, terms both on the left-hand-side of Equation (18), are treated using the hybrid differencing scheme. The non-orthogonal diffusion terms on the right-hand-side of Equation (18) are evaluated using a linear ϕ profile and lumped into the source term. The resulting discretization equation for the dependent variable ϕ can be written in the following general form

$$A_{\mathrm{P}}\phi_{\mathrm{P}}=A_{\mathrm{E}}\phi_{\mathrm{E}}+A_{\mathrm{W}}\phi_{\mathrm{W}}+A_{\mathrm{N}}\phi_{\mathrm{N}}+A_{\mathrm{S}}\phi_{\mathrm{S}}+A_{\mathrm{T}}\phi_{\mathrm{T}}+A_{\mathrm{B}}\phi_{\mathrm{B}}+b^{\phi}, \tag{19}$$

where the subscripts P and E, W, N, S, T, B denote the main grid node and its neighboring nodes on the east, west, north, south, top and bottom, respectively.

4.1. Discretization of continuity equation

Setting $\phi=1$ and $\mathrm{S}^{\phi}=0$ in Equation (18), gives the following discretized continuity equation

$$[U^1\Delta\xi^2\Delta\xi^3]_{\mathrm{e}}-[U^1\Delta\xi^2\Delta\xi^3]_{\mathrm{w}}+[U^2\Delta\xi^1\Delta\xi^3]_{\mathrm{n}}-[U^2\Delta\xi^1\Delta\xi^3]_{\mathrm{s}}+[U^3\Delta\xi^1\Delta\xi^2]_{\mathrm{t}}-[U^3\Delta\xi^1\Delta\xi^2]_{\mathrm{b}}=0. \tag{20}$$

4.2. Discretization of momentum equations

Having the discretization equation for ϕ (Equation (19)), the discretization equations for the Cartesian velocity components, u_j, ($j=1, 2, 3$) can be obtained.

$$A_{\mathrm{P}}(u_j)_{\mathrm{P}}=A_{\mathrm{E}}(u_j)_{\mathrm{E}}+A_{\mathrm{W}}(u_j)_{\mathrm{W}}+A_{\mathrm{N}}(u_j)_{\mathrm{N}}+A_{\mathrm{S}}(u_j)_{\mathrm{S}}+A_{\mathrm{T}}(u_j)_{\mathrm{T}}+A_{\mathrm{B}}(u_j)_{\mathrm{B}}+b^{u_j}. \tag{21}$$

The expressions for the coefficients A_{P}, A_{E}, ..., A_{B} and the source term b^{u_j} can be found in Appendix A.

The discretization equations for the contravariant velocity fluxes U^i can be obtained by multiplying the discretization equations for $(u_j)_{\mathrm{P}}$ by $(\bar{J}_j^i\rho)_{\mathrm{P}}$ and adding them up

$$A_{\mathrm{P}}(U^i)_{\mathrm{P}}=A_{\mathrm{E}}(U^i)_{\mathrm{E}}^0+A_{\mathrm{W}}(U^i)_{\mathrm{W}}^0+A_{\mathrm{N}}(U^i)_{\mathrm{N}}^0+A_{\mathrm{S}}(U^i)_{\mathrm{S}}^0+A_{\mathrm{T}}(U^i)_{\mathrm{T}}^0+A_{\mathrm{B}}(U^i)_{\mathrm{B}}^0+b^{U^i}, \tag{22}$$

where

$$(U^i)_{\mathrm{E}}^0=(\bar{J}_j^i\rho)_{\mathrm{P}}(u_j)_{\mathrm{E}}, \tag{23}$$

$$(b)^{U^i}=(\bar{J}_j^i\rho)_{\mathrm{P}}b^{u_j}. \tag{24}$$

Similar expressions can be written for the $(U^i)_{\mathrm{W}}^0$, $(U^i)_{\mathrm{N}}^0$, $(U^i)_{\mathrm{S}}^0$, $(U^i)_{\mathrm{T}}^0$ and $(U^i)_{\mathrm{B}}^0$. Equation (22) would not have a solution because different variables exist on the two sides of the equation. This difficulty can be overcome by introducing the 'actual' neighbor [2] as follows

$$A_{\mathrm{P}}(U^i)_{\mathrm{P}}=A_{\mathrm{E}}(U^i)_{\mathrm{E}}+A_{\mathrm{W}}(U^i)_{\mathrm{W}}+A_{\mathrm{N}}(U^i)_{\mathrm{N}}+A_{\mathrm{S}}(U^i)_{\mathrm{S}}+A_{\mathrm{T}}(U^i)_{\mathrm{T}}+A_{\mathrm{B}}(U^i)_{\mathrm{B}}+b^{U^i}+b_{\mathrm{CURV}}^{U^i}, \tag{25}$$

where

$$b^{U^i}_{\mathrm{CURV}} = A_{\mathrm{E}}[(U^i)^0_{\mathrm{E}} - (U^i)_{\mathrm{E}}] + A_{\mathrm{W}}[(U^i)^0_{\mathrm{W}} - (U^i)_{\mathrm{W}}] + A_{\mathrm{N}}[(U^i)^0_{\mathrm{N}} - (U^i)_{\mathrm{N}}] + A_{\mathrm{S}}[(U^i)^0_{\mathrm{S}} - (U^i)_{\mathrm{S}}] + A_{\mathrm{T}}[(U^i)^0_{\mathrm{T}} - (U^i)_{\mathrm{T}}] + A_{\mathrm{B}}[(U^i)^0_{\mathrm{B}} - (U^i)_{\mathrm{B}}]. \tag{26}$$

Equation (25) is the discretized momentum equation using the contravariant velocity fluxes as the dependent variables and it retains a strongly conservative form. Equation (25) is solved together with Equation (20). For the convenience of the derivation in the subsequent sections, Equation (25) is rewritten as

$$A_{\mathrm{P}}(U^i)_{\mathrm{P}} = \sum A_{nb}(U^i)_{nb} + (B^{ij})_{\mathrm{P}}\left(\frac{\partial p}{\partial \xi^j}\right)_{\mathrm{P}} + b^{U^i}_{n\mathrm{P}}, \tag{27}$$

where the subscript *nb* runs over the six nearest neighbors of the node P, namely, E, W, N, S, T and B. $b^{U^i}_{n\mathrm{P}}$ denotes all the source terms except the pressure gradient terms, and is expressed as

$$b^{U^i}_{n\mathrm{P}} = b^{U^i} + b^{U^i}_{\mathrm{CURV}} - (B^{ij})_{\mathrm{P}}\left(\frac{\partial p}{\partial \xi^j}\right)_{\mathrm{P}}. \tag{28}$$

B^{ij} is given by

$$B^{ij} = -\rho \bar{J}^i_k J^j_k \Delta\xi^1 \Delta\xi^2 \Delta\xi^3. \tag{29}$$

5. MOMENTUM INTERPOLATION SCHEMES

Although the non-staggered grid arrangement is attractive due to its simplicity for the locations of the variables, the drawback of this arrangement is the occurrence of the non-physical oscillations of the pressure and/or velocity fields. This is due to the fact that the resulting equations couple the pressure and the velocities at alternate nodes only, if a linear interpolation is used to express the internodal pressure gradients in the momentum equations and the velocity variation in the continuity equation. In order to suppress oscillations, a special interpolation practice called momentum interpolation is adopted. In this practice, the velocities at the cell face are calculated by 'algebraically' using the discretized momentum equations for two adjacent nodes instead of solving the discretized momentum equations for the node at the cell face as done in the staggered grid arrangement. In this section, different formulations of the momentum interpolation in general curvilinear co-ordinates are presented.

The cross pressure gradient terms exist in Equation (27). However, the main pressure gradient terms are separated from the source terms and the cross terms are lumped into the source terms when the momentum interpolation scheme is adopted. Divided by A_{P}, Equation (27) can be written in a more compact form

$$(U^i)_{\mathrm{P}} = (H_{U^i})_{\mathrm{P}} + (C^{ii})_{\mathrm{P}}\left(\frac{\partial p}{\partial \xi^i}\right)_{\mathrm{P}} \quad \text{for node P}, \tag{30a}$$

$$(U^i)_{\mathrm{P}+1} = (H_{U^i})_{\mathrm{P}+1} + (C^{ii})_{\mathrm{P}+1}\left(\frac{\partial p}{\partial \xi^i}\right)_{\mathrm{P}+1} \quad \text{for node P} + 1, \tag{30b}$$

where H_{U^i} is the summation of all the terms except the main pressure gradient term and is given by

$$H_{U^i} = \left[\sum A_{nb}(U^i)_{nb} + (B^{ij})\left(\frac{\partial p}{\partial \xi^j}\right) + b_{n\mathrm{P}}^{U^i} - (B^{ii})\left(\frac{\partial p}{\partial \xi^i}\right) \right] \Big/ A_{\mathrm{P}}. \tag{31}$$

Node P + 1 is the neighboring node of P, namely, E, N or T. C^{ii} is given by

$$C^{ii} = \frac{B^{ii}}{A_{\mathrm{P}}}. \tag{32}$$

Here, B^{ii} and A_{P} are treated as a whole. It is noted here that there is no summation over the index i for all equations in this section.

Usually, an underrelaxation factor is introduced into the discretization equation to ensure the convergence. Hence, Equation (30a) can be written as

$$(U^i)_{\mathrm{P}} = \alpha_{U^i}\left[(H_{U^i})_{\mathrm{P}} + (C^{ii})_{\mathrm{P}}\left(\frac{\partial p}{\partial \xi^i}\right)_{\mathrm{P}} \right] + (1-\alpha_{U^i})(U^i)_{\mathrm{P}}^{(n-1)} = (h_{U^i})_{\mathrm{P}} + \alpha_{U^i}(C^{ii})_{\mathrm{P}}\left(\frac{\partial p}{\partial \xi^i}\right)_{\mathrm{P}}, \tag{33}$$

where α_{U^i} is the velocity underrelaxation factor, $(U^i)^{(n-1)}$ is the value of U^i at the level of last iteration, and

$$(h_{U^i})_{\mathrm{P}} = \alpha_{U^i}(H_{U^i})_{\mathrm{P}} + (1-\alpha_{U^i})(U^i)_{\mathrm{P}}^{(n-1)}. \tag{34}$$

Similarly, Equation (30b) can be written as

$$(U^i)_{\mathrm{P}+1} = (h_{U^i})_{\mathrm{P}+1} + \alpha_{U^i}(C^{ii})_{\mathrm{P}+1}\left(\frac{\partial p}{\partial \xi^i}\right)_{\mathrm{P}+1}, \tag{35}$$

where

$$(h_{U^i})_{\mathrm{P}+1} = \alpha_{U^i}(H_{U^i})_{\mathrm{P}+1} + (1-\alpha_{U^i})(U^i)_{\mathrm{P}+1}^{(n-1)}. \tag{36}$$

One way to carry out the momentum interpolation scheme is to write the discretization equation at the cell face P + 1/2 (P + 1/2 denotes the cell faces e, n or t) as

$$(U^i)_{\mathrm{P}+1/2} = [f^+(h_{U^i})_{\mathrm{P}+1} + (1-f^+)(h_{U^i})_{\mathrm{P}}] + \alpha_{U^i}(C^{ii})_{\mathrm{P}+1/2}\left(\frac{\partial p}{\partial \xi^i}\right)_{\mathrm{P}+1/2}, \tag{37}$$

where f^+ is the geometric interpolation factor and is given by

$$f^+ = \frac{d_{(\mathrm{P})(\mathrm{P}+1/2)}}{d_{(\mathrm{P})(\mathrm{P}+1/2)} + d_{(\mathrm{P}+1/2)(\mathrm{P}+1)}}, \tag{38}$$

where $d_{(\mathrm{P})(\mathrm{P}+1/2)}$ stands for the distance between the node P and the face P + 1/2, while $d_{(\mathrm{P}+1/2)(\mathrm{P}+1)}$ is the distance between the face P + 1/2 and the node P + 1. In Equation (37), $(C^{ii})_{\mathrm{P}+1/2}$ can be evaluated by a linear interpolation of $(C^{ii})_{\mathrm{P}}$ and $(C^{ii})_{\mathrm{P}+1}$. $(\partial \mathrm{P}/\partial \xi^i)_{\mathrm{P}+1/2}$ can be discretized using the nodes P and P + 1. Majumdar [5] has shown that using such a momentum interpolation formulation (Equation (37)) will not lead to a unique solution for a given flow field in Cartesian co-ordinates. This is because the solution depends on the underrelaxation factor α_{U^i}. Our computational results also confirm this in general curvilinear co-ordinates. Therefore, Equation (37) should be discarded.

Another way to evaluate the U^i value at the face P + 1/2 is to carry out the underrelaxation explicitly, namely

$$(U^i)_{\mathrm{P}+1/2} = \alpha_{U^i}\left[(\overline{H_{U^i}}) + (C^{ii})_{\mathrm{P}+1/2}\left(\frac{\partial p}{\partial \xi^i}\right)_{\mathrm{P}+1/2} \right] + (1-\alpha_{U^i})(U^i)_{\mathrm{P}+1/2}^{(n-1)}, \tag{39}$$

where

$$\overline{H_{U^i}} = f^+(H_{U^i})_{\mathrm{P}+1} + (1-f^+)(H_{U^i})_{\mathrm{P}}. \tag{40}$$

In Cartesian co-ordinates, Majumdar [5] has shown that such implementation of the momentum interpolation can result in a unique solution for a given flow field. Our computation experience also confirms this in general curvilinear co-ordinates. In the present work, this formulation is adopted to be a starting point for further derivation.

There are two practices for evaluating (H_{U^i}) and $(H_{U^i})_{\mathrm{P}+1}$. One practice to calculate the values of $(H_{U^i})_{\mathrm{P}}$ and $(H_{U^i})_{\mathrm{P}+1}$ is to use Equation (31). Substituting Equation (31) into (40) and then (39) gives

$$\begin{aligned}(U^i)_{\mathrm{P}+1/2} = \alpha_{U^i}\Bigg[& f^+\left(\sum A_{nb}(U^i)_{nb} + (B^{ij})\left(\frac{\partial p}{\partial \xi^j}\right) + b_{n\mathrm{P}}^{U^i} - (B^{ii})\left(\frac{\partial p}{\partial \xi^i}\right)\right)_{\mathrm{P}+1} \Big/ A_{\mathrm{P}+1} \\ & + (1-f^+)\left(\sum A_{nb}(U^i)_{nb} + (B^{ij})\left(\frac{\partial p}{\partial \xi^j}\right) + b_{n\mathrm{P}}^{U^i} - (B^{ii})\left(\frac{\partial p}{\partial \xi^i}\right)\right)_{\mathrm{P}} \Big/ A_{\mathrm{P}} \\ & + (C^{ii})_{\mathrm{P}+1/2}\left(\frac{\partial p}{\partial \xi^i}\right)_{\mathrm{P}+1/2}\Bigg] + (1-\alpha_{U^i})(U^i)_{\mathrm{P}+1/2}^{(n-1)}. \end{aligned} \tag{41}$$

This practice is denoted as Practice A in the present work. Equation (41) is the expression for $(U^i)_{\mathrm{P}+1/2}$. In another practice, the values of $(H_{U^i})_{\mathrm{P}}$ and $(H_{U^i})_{\mathrm{P}+1}$ are calculated based on Equations (30a) and (30b). That is

$$(H_{U^i})_{\mathrm{P}} = (U^i)_{\mathrm{P}} - (C^{ii})_{\mathrm{P}}\left(\frac{\partial p}{\partial \xi^i}\right)_{\mathrm{P}}, \tag{42a}$$

and

$$(H_{U^i})_{\mathrm{P}+1} = (U^i)_{\mathrm{P}+1} - (C^{ii})_{\mathrm{P}+1}\left(\frac{\partial p}{\partial \xi^i}\right)_{\mathrm{P}+1}. \tag{42b}$$

Substituting these two equations into Equation (40) and then (39) gives

$$\begin{aligned}(U^i)_{\mathrm{P}+1/2} = \alpha_{U^i}\Bigg[& f^+(U^i)_{\mathrm{P}+1} + (1-f^+)(U^i)_{\mathrm{P}} + (C^{ii})_{\mathrm{P}+1/2}\left(\frac{\partial p}{\partial \xi^i}\right)_{\mathrm{P}+1/2} - f^+(C^{ii})_{\mathrm{P}+1}\left(\frac{\partial p}{\partial \xi^i}\right)_{\mathrm{P}+1} \\ & - (1-f^+)(C^{ii})_{\mathrm{P}}\left(\frac{\partial p}{\partial \xi^i}\right)_{\mathrm{P}}\Bigg] + (1-\alpha_{U^i})(U^i)_{\mathrm{P}+1/2}^{(n-1)}. \end{aligned} \tag{43}$$

This practice is denoted as Practice B in the present work and Equation (43) is its expression for $(U^i)_{\mathrm{P}+1/2}$. In short, the difference between the two Practices is how to evaluate $(H_{U^i})_{\mathrm{P}}$ and $(H_{U^i})_{\mathrm{P}+1}$, which result in different expressions for $(U^i)_{\mathrm{P}+1/2}$, i.e. Equation (41) for Practice A and Equation (43) for Practice B. In Equation (41) the velocity values and the coefficients are used before the solver is called to solve the nodal momentum equations. In Equation (43), the new velocity values are used after the solver is called. This could influence the convergence behavior as shown in the companion paper [12].

Both Equation (41) (Practice A) and Equation (43) (Practice B) have velocity underrelaxation factors in them. To make these two equations simpler, α_{U^i} can be set to 1. Thus, Equations (41) and (43) become

$$(U^i)_{P+1/2} = f^+\left(\sum A_{nb}(U^i)_{nb} + (B^{ij})\left(\frac{\partial p}{\partial \xi^j}\right) + b_{nP}^{U^i} - (B^{ii})\left(\frac{\partial p}{\partial \xi^i}\right)\right)_{P+1} \Big/ A_{P+1}$$
$$+ (1-f^+)\left(\sum A_{nb}(U^i)_{nb} + (B^{ij})\left(\frac{\partial p}{\partial \xi^j}\right) + b_{nP}^{U^i} - (B^{ii})\left(\frac{\partial p}{\partial \xi^i}\right)\right)_{P} \Big/ A_P$$
$$+ (C^{ii})_{P+1/2}\left(\frac{\partial p}{\partial \xi^i}\right)_{P+1/2}, \tag{44}$$

and

$$(U^i)_{P+1/2} = f^+(U^i)_{P+1} + (1-f^+)(U^i)_P + (C^{ii})_{P+1/2}\left(\frac{\partial p}{\partial \xi^i}\right)_{P+1/2} - f^+(C^{ii})_{P+1}\left(\frac{\partial p}{\partial \xi^i}\right)_{P+1}$$
$$- (1-f^+)(C^{ii})_P\left(\frac{\partial p}{\partial \xi^i}\right)_P. \tag{45}$$

Equations (41) and (43) and Equations (44) and (45) are momentum interpolation formulations for Practice A and Practice B with and without the velocity underrelaxation factor, α_{U^i}, respectively. The velocity underrelaxation factor α_{U^i} in the discretized momentum equations (Equation (33)) is always retained, no matter which momentum interpolation formulation is used. However, the value of α_{U^i} in the momentum interpolation formulation is set to be identical with that in the discretized momentum equations if a momentum interpolation formulation with α_{U^i}, i.e. Equation (41) or (43), is used.

If $(C^{ii})_P$ and $(C^{ii})_{P+1}$, are assumed to be approximately equal to $(C^{ii})_{P+1/2}$, Equation (45) becomes the Rhie and Chow's momentum interpolation formulation [4]. Furthermore, Equation (45) can be considered as an extension of Miller and Schmidt's formulation [6] to the general curvilinear co-ordinates. It is noted that using these two practices either with α_{U^i}, or without α_{U^i} can always result in the same solution for a given flow field, no matter what value for α_{U^i} is used, and Rhie and Chow's formulation also leads to a unique solution. However, these two solutions are different in accuracy due to the approximation made by setting $(C^{ii})_P$ and $(C^{ii})_{P+1}$ in Equation (45) to be $(C^{ii})_{P+1/2}$ in Rhie and Chow's formulation respectively. Obviously, the accuracy of Rhie and Chow's formulation is lower than that of Equation (45). In the present work, both Practice A and Practice B with and without α_{U^i}, are tested to show their abilities to give a converged solution on non-orthogonal grids.

6. TREATMENT OF THE PRESSURE–VELOCITY COUPLING

The coupling between the momentum equations and the continuity equation is done by using the SIMPLE [13], SIMPLEC [14] and SIMPLER [15] algorithms. These three algorithms are combined with Practice A and Practice B to solve the governing equations, respectively.

The resulting velocity field from the momentum equations generally does not satisfy the continuity equation unless the correct pressure field is employed. Such an imperfect velocity field based on the imperfect pressure field p^* is denoted by $(U^i)^*$. This 'starred', velocity field results from the solution of Equation (27)

$$A_P(U^i)_P^* = \sum A_{nb}(U^i)_{nb}^* + (B^{ij})_P\left(\frac{\partial p^*}{\partial \xi^j}\right)_P + b_{nP}^{U^i}. \tag{46}$$

In both SIMPLE and SIMPLEC algorithms, p^* is initiated by guessing its value, while in SIMPLER algorithm it is initiated by solving a Poisson-like equation based on the continuity equation. The velocity correction can be expressed as

$$(U^i)'_{\mathrm{P}} = (\hat{B}^{ij})_{\mathrm{P}}\left(\frac{\partial p'}{\partial \xi^j}\right)_{\mathrm{P}}. \tag{47}$$

Equation (47) is obtained by first subtracting Equation (46) from (27) and then making some assumptions according to the SIMPLE series algorithms. $\hat{B}^{ij}$ is a coefficient and it is different for different algorithms. Its full expression can be found in Appendix B. p' is the pressure correction. The corrected velocity field is given by

$$U^i = (U^i)^* + (U^i)' = (U^i)^* + \hat{B}^{ij}\frac{\partial p'}{\partial \xi^j}. \tag{48}$$

Substituting Equation (48) into the continuity equation (Equation (20)) gives the following pressure correction equations

$$A_{\mathrm{P}}p'_{\mathrm{P}} = \sum A_{nb}p'_{nb} + S_{\mathrm{P}}, \tag{49}$$

where

$$A_{\mathrm{E}} = \left(\frac{\hat{B}^{11}\Delta\xi^2\Delta\xi^3}{\Delta\xi^1}\right)_{\mathrm{e}}, \qquad A_{\mathrm{N}} = \left(\frac{\hat{B}^{22}\Delta\xi^1\Delta\xi^3}{\Delta\xi^2}\right)_{\mathrm{n}}, \qquad A_{\mathrm{T}} = \left(\frac{\hat{B}^{33}\Delta\xi^1\Delta\xi^2}{\Delta\xi^3}\right)_{\mathrm{t}},$$

$$A_{\mathrm{P}} = \sum A_{nb}, \tag{50}$$

$$S_{\mathrm{P}} = m_{\mathrm{P}} + S_{\mathrm{NO}}. \tag{51}$$

The coefficients A_{W}, A_{S}, and A_{B} can be expressed in a similar way as A_{E}, A_{N} and A_{T}. In Equation (51), m_{P} is calculated by Equation (20) with U^i replaced by $(U^i)^*$, and

$$S_{\mathrm{NO}} = \left[\left(\hat{B}^{12}\frac{\partial p'}{\partial \xi^2} + \hat{B}^{13}\frac{\partial p'}{\partial \xi^3}\right)\Delta\xi^2\Delta\xi^3\right]_{\mathrm{w}}^{\mathrm{e}} + \left[\left(\hat{B}^{21}\frac{\partial p'}{\partial \xi^1} + \hat{B}^{23}\frac{\partial p'}{\partial \xi^3}\right)\Delta\xi^1\Delta\xi^3\right]_{\mathrm{s}}^{\mathrm{n}} + \left[\left(\hat{B}^{31}\frac{\partial p'}{\partial \xi^1} + \hat{B}^{32}\frac{\partial p'}{\partial \xi^2}\right)\Delta\xi^1\Delta\xi^2\right]_{\mathrm{b}}^{\mathrm{t}}. \tag{52}$$

In the present study, the non-orthogonal term S_{NO} is omitted in order to simplify the pressure correction equation. Hence, Equation (49) has a seven-nodal coefficient matrix. After Equation (49) is solved, the velocity field is corrected using Equation (48). In both SIMPLE and SIMPLEC algorithms, the pressure field is corrected by

$$p = p^* + \alpha_p p', \tag{53}$$

where α_p is the pressure underrelaxation factor. For the SIMPLE algorithm, α_p is usually < 1. For the SIMPLEC algorithm, it could be 1. In the SIMPLER algorithm, p is corrected by solving a Poisson-like equation based on the continuity equation, which is very similar to Equation (49). In this Poisson-like equation, p' is replaced by p, m_p is calculated using the pseudovelocities, and S_{NO} can be treated explicitly.

7. CONCLUDING REMARKS

In this article, the contravariant velocity fluxes were used as the dependent variables in the momentum equations in body fitted co-ordinates. The discretization equations for contravariant velocity fluxes were derived from those for Cartesian velocity components and retain a

strongly conservative form. The hybrid differencing scheme was employed to discretize the convection and orthogonal diffusion terms in the momentum equations. The non-staggered grid arrangement was adopted. Two different practices for treating the momentum interpolation, namely Practice A and Practice B, were presented. In each practice, the momentum interpolation formulations with and without a velocity underrelaxation factor were considered. The formulation of Practice B can be reduced to the Rhie and Chow's formulation [4] if some simplifications are made. Also, Practice B can be considered as an extension of Miller and Schmidt's formulation [6]. The coupling between the momentum equations and the continuity equation was done using the SIMPLE, SIMPLEC and SIMPLER algorithms, respectively. The non-orthogonal terms in the pressure correction equation were omitted. Each of these three algorithms is to be combined with Practice A and Practice B to study the effect of the grid non-orthogonality by solving the typical cavity flows. The results are given in a companion article [12].

APPENDIX A

In the present study, the hybrid differencing scheme is used to discretize the convection and orthogonal diffusion terms. Therefore, the coefficients A_E, A_W, A_N, A_S, A_T, A_B and A_P in Equation (21) are expressed as

$$\begin{aligned}
&A_E = D_e A(|Pe_e|) + (|-F_e, 0|), \qquad A_W = D_w A(|Pe_w|) + (|F_w, 0|),\\
&A_N = D_n A(|Pe_n|) + (|-F_n, 0|), \qquad A_S = D_s A(|Pe_s|) + (|F_s, 0|),\\
&A_T = D_t A(|Pe_t|) + (|-F_t, 0|), \qquad A_B = D_b A(|Pe_b|) + (|F_b, 0|),\\
&A_P = A_E + A_W + A_N + A_S + A_T + A_B,
\end{aligned} \tag{A1}$$

where

$$A(|Pe_e|) = \max(0, 1.0, -0.5|Pe_e|). \tag{A2}$$

Similar expressions can be written for $A(|Pe_w|)$, $A(|Pe_n|)$, $A(|Pe_s|)$, $A(|Pe_t|)$ and $A(|Pe_b|)$. In Equation (A1), F_e, F_w, F_n, F_s, F_t and F_b are the flow fluxes through the cell faces e, w, n, s, t and b, respectively. They are written as

$$\begin{aligned}
&F_e = [U^1 \Delta\xi^2 \Delta\xi^3]_e, \qquad F_w = [U^1 \Delta\xi^2 \Delta\xi^3]_w, \qquad F_n = [U^2 \Delta\xi^3 \Delta\xi^1]_n,\\
&F_s = [U^2 \Delta\xi^3 \Delta\xi^1]_s, \qquad F_t = [U^3 \Delta\xi^1 \Delta\xi^2]_t, \qquad F_b = [U^3 \Delta\xi^1 \Delta\xi^2]_b.
\end{aligned} \tag{A3}$$

D_e, D_w, D_n, D_s, D_t and D_b are the orthogonal diffusion conductances and are written as

$$\begin{aligned}
&D_e = \left[\frac{\bar{J}_k^1 \bar{J}_k^1 \Gamma \Delta\xi^2 \Delta\xi^3}{Ja\delta\xi^1}\right]_e, \qquad D_w = \left[\frac{\bar{J}_k^1 \bar{J}_k^1 \Gamma \Delta\xi^2 \Delta\xi^3}{Ja\delta\xi^1}\right]_w, \qquad D_n = \left[\frac{\bar{J}_k^2 \bar{J}_k^2 \Gamma \Delta\xi^1 \Delta\xi^3}{Ja\delta\xi^2}\right]_n,\\
&D_s = \left[\frac{\bar{J}_k^2 \bar{J}_k^2 \Gamma \Delta\xi^1 \Delta\xi^3}{Ja\delta\xi^2}\right]_s, \qquad D_t = \left[\frac{\bar{J}_k^3 \bar{J}_k^3 \Gamma \Delta\xi^1 \Delta\xi^2}{Ja\delta\xi^3}\right]_t, \qquad D_b = \left[\frac{\bar{J}_k^3 \bar{J}_k^3 \Gamma \Delta\xi^1 \Delta\xi^2}{Ja\delta\xi^3}\right]_b.
\end{aligned} \tag{A4}$$

Pe is the Peclet number, which, for example at the cell face e, is defined as

$$Pe_{\mathrm{e}} = \frac{F_{\mathrm{e}}}{D_{\mathrm{e}}}. \tag{A5}$$

Similar definitions are applied to the Pe on the cell faces at w, n, s, t and b.

The source term b^{u_j} in Equation (21) is expressed as

$$\begin{aligned} b^{u_j} = {} & (D_{\mathrm{e1}} - D_{\mathrm{w1}} + D_{\mathrm{t2}} - D_{\mathrm{b2}})(u_j)_{\mathrm{N}} + (D_{\mathrm{w1}} - D_{\mathrm{e1}} + D_{\mathrm{b2}} - D_{\mathrm{t2}})(u_j)_{\mathrm{S}} \\ & + (D_{\mathrm{n1}} - D_{\mathrm{s1}} + D_{\mathrm{t1}} - D_{\mathrm{b1}})(u_j)_{\mathrm{E}} + (D_{\mathrm{s1}} - D_{\mathrm{n1}} + D_{\mathrm{b1}} - D_{\mathrm{t1}})(u_j)_{\mathrm{W}} \\ & + (D_{\mathrm{n2}} - D_{\mathrm{s2}} + D_{\mathrm{e2}} - D_{\mathrm{w2}})(u_j)_{\mathrm{T}} + (D_{\mathrm{s2}} - D_{\mathrm{n2}} + D_{\mathrm{w2}} - D_{\mathrm{e2}})(u_j)_{\mathrm{B}} \\ & + A_{\mathrm{NE}}(u_j)_{\mathrm{NE}} + A_{\mathrm{NW}}(u_j)_{\mathrm{NW}} + A_{\mathrm{SE}}(u_j)_{\mathrm{SE}} + A_{\mathrm{SW}}(u_j)_{\mathrm{SW}} + A_{\mathrm{ET}}(u_j)_{\mathrm{ET}} + A_{\mathrm{WT}}(u_j)_{\mathrm{WT}} \\ & + A_{\mathrm{NT}}(u_j)_{\mathrm{NT}} + A_{\mathrm{ST}}(u_j)_{\mathrm{ST}} + A_{\mathrm{EB}}(u_j)_{\mathrm{EB}} + A_{\mathrm{WB}}(u_j)_{\mathrm{WB}} + A_{\mathrm{SB}}(u_j)_{\mathrm{SB}} + A_{\mathrm{NB}}(u_j)_{\mathrm{NB}}, \end{aligned} \tag{A6}$$

where D_{e1}, $D_{\mathrm{w1}}, \ldots,$ are the non-orthogonal diffusion conductances and are given by

$$\begin{aligned} & D_{\mathrm{e1}} = \left[\frac{\bar{J}_k^2 \bar{J}_k^1 \Gamma \Delta\xi^2 \Delta\xi^3}{4Ja\delta\xi^2}\right]_{\mathrm{e}}, \quad D_{\mathrm{w1}} = \left[\frac{\bar{J}_k^2 \bar{J}_k^1 \Gamma \Delta\xi^2 \Delta\xi^3}{4Ja\delta\xi^2}\right]_{\mathrm{w}}, \quad D_{\mathrm{e2}} = \left[\frac{\bar{J}_k^3 \bar{J}_k^1 \Gamma \Delta\xi^2 \Delta\xi^3}{4Ja\delta\xi^3}\right]_{\mathrm{e}}, \\ & D_{\mathrm{w2}} = \left[\frac{\bar{J}_k^3 \bar{J}_k^1 \Gamma \Delta\xi^2 \Delta\xi^3}{4Ja\delta\xi^3}\right]_{\mathrm{w}}, \quad D_{\mathrm{n1}} = \left[\frac{\bar{J}_k^1 \bar{J}_k^2 \Gamma \Delta\xi^1 \Delta\xi^3}{4Ja\delta\xi^1}\right]_{\mathrm{n}}, \quad D_{\mathrm{s1}} = \left[\frac{\bar{J}_k^1 \bar{J}_k^2 \Gamma \Delta\xi^1 \Delta\xi^3}{4Ja\delta\xi^1}\right]_{\mathrm{s}}, \\ & D_{\mathrm{n2}} = \left[\frac{\bar{J}_k^3 \bar{J}_k^2 \Gamma \Delta\xi^1 \Delta\xi^3}{4Ja\delta\xi^3}\right]_{\mathrm{n}}, \quad D_{\mathrm{s2}} = \left[\frac{\bar{J}_k^3 \bar{J}_k^2 \Gamma \Delta\xi^1 \Delta\xi^3}{4Ja\delta\xi^3}\right]_{\mathrm{s}}, \quad D_{\mathrm{t1}} = \left[\frac{\bar{J}_k^1 \bar{J}_k^3 \Gamma \Delta\xi^1 \Delta\xi^2}{4Ja\delta\xi^1}\right]_{\mathrm{t}}, \\ & D_{\mathrm{b1}} = \left[\frac{\bar{J}_k^1 \bar{J}_k^3 \Gamma \Delta\xi^1 \Delta\xi^2}{4Ja\delta\xi^1}\right]_{\mathrm{b}}, \quad D_{\mathrm{t2}} = \left[\frac{\bar{J}_k^2 \bar{J}_k^3 \Gamma \Delta\xi^1 \Delta\xi^2}{4Ja\delta\xi^2}\right]_{\mathrm{t}}, \quad D_{\mathrm{b2}} = \left[\frac{\bar{J}_k^2 \bar{J}_k^3 \Gamma \Delta\xi^1 \Delta\xi^2}{4Ja\delta\xi^2}\right]_{\mathrm{b}}, \end{aligned} \tag{A7}$$

and

$$\begin{aligned} & A_{\mathrm{NE}} = D_{\mathrm{n1}} + D_{\mathrm{e1}}, \quad A_{\mathrm{NW}} = -(D_{\mathrm{n1}} + D_{\mathrm{w1}}), \quad A_{\mathrm{SE}} = -(D_{\mathrm{s1}} + D_{\mathrm{e1}}), \\ & A_{\mathrm{SW}} = D_{\mathrm{s1}} + D_{\mathrm{w1}}, \quad A_{\mathrm{ET}} = D_{\mathrm{e2}} + D_{\mathrm{t1}}, \quad A_{\mathrm{WT}} = -(D_{\mathrm{t1}} + D_{\mathrm{w2}}), \\ & A_{\mathrm{NT}} = D_{\mathrm{n2}} + D_{\mathrm{t2}}, \quad A_{\mathrm{ST}} = -(D_{\mathrm{t2}} + D_{\mathrm{s2}}), \quad A_{\mathrm{EB}} = -(D_{\mathrm{b1}} + D_{\mathrm{e2}}), \\ & A_{\mathrm{WB}} = D_{\mathrm{w2}} + D_{\mathrm{b1}}, \quad A_{\mathrm{SB}} = D_{\mathrm{b2}} + D_{\mathrm{s2}}, \quad A_{\mathrm{NB}} = -(D_{\mathrm{n2}} + D_{\mathrm{b2}}). \end{aligned} \tag{A8}$$

The non-orthogonal diffusion conductances are zero in orthogonal co-ordinates.

APPENDIX B

In the SIMPLE [13] and SIMPLER [15] algorithms, the coefficient $(\hat{B}^{ij})_{\mathrm{P}}$ in Equation (46) is written as

$$\hat{B}^{ij} = \frac{(B^{ij})_{\mathrm{P}}}{A_{\mathrm{P}}}. \tag{B1}$$

In the SIMPLEC [14] algorithm, this coefficient is written as

$$\hat{B}^{ij} = \frac{(B^{ij})_{\mathrm{P}}}{A_{\mathrm{P}} - \sum A_{nb}}. \tag{B2}$$

However, the denominator $A_{\mathrm{P}} - \Sigma A_{nb}$ is zero according to Equation (A1). Fortunately, this can be avoided when the underrelaxation factor α_{U^i} is introduced into the momentum nodal equations to ensure the convergence, as shown in Equation (33). Thus, Equation (B2) becomes

$$\hat{B}^{ij} = \frac{(B^{ij})_{\mathrm{P}}}{A_{\mathrm{P}}/\alpha_{U^i} - \sum A_{nb}}. \tag{B3}$$

Since $0 < \alpha_{U^i} < 1.0$, $A_{\mathrm{P}}/\alpha_{U^i} - \Sigma A_{nb}$ is always greater than 0.

NOMENCLATURE

A	coefficient in the discretized equations
b	source term in the discretized equations
B^{ij}, $\hat{B}^{ij}$, C^{ij}	coefficients of the pressure gradient terms
d	distance between the node and the cell face
D	diffusion conductance
e_i	covariant base vector
f^+	geometric interpolation factor
F	flow flux
h	given by Equation (32)
H	all the terms on the right-hand-side of the discretized momentum equations except the main pressure gradient term
$\boldsymbol{i}_i$	Cartesian unit vector
$\boldsymbol{J}$	convective and diffusive flux vector
J^{x^i}	Cartesian component of $\boldsymbol{J}$
J^{ξ^i}	curvilinear component of $\boldsymbol{J}$
$\bar{J}$	defined by Equation (13)
Ja	Jacobian of the transformation
m_{P}	mass residual in the discretized P' equation
p	pressure
Pe	Peclet number
S	source term in the governing equation and in the discretized p' equation
$\boldsymbol{u}$	velocity vector
u_i	Cartesian velocity component
U^i	contravariant velocity flux
V^i	contravariant velocity component
x^i	Cartesian co-ordinates
α_{U^i}	velocity underrelaxation factor
α_p	pressure underrelaxation factor
δ	nodal difference
Δ	control volume difference
ϕ	general dependent variable

Γ	diffusivity
μ	dynamic viscosity
ξ^i	general curvilinear co-ordinates
ρ	density

Indices

i, j, k	co-ordinate direction identifiers

Subscripts

e, w, n, s, t, b	values at the cell faces
E, W, N, S, T, B	values at the nodal points
P	main nodal point

Superscripts

*	uncorrected values
′	corrected values

REFERENCES

1. J.F. Thompson, Z.U.A. Warsi and C.W. Mastin, *Numerical Grid Generation, Foundations and Applications*, North-Holland, New York, 1985.
2. K.C. Karki, 'A calculation procedure for viscous flows at all speeds in complex geometries', *Ph.D. Thesis*, University of Minnesota, Minneapolis, 1986.
3. H.Q. Yang, S.D. Habchi and A.J. Przekwas, 'General strong conservation formulation of Navier–Stokes equations in nonorthogonal curvilinear coordinates', *AIAA J.*, **32**, 936–941 (1994).
4. C.M. Rhie and W.L. Chow, 'Numerical study of the turbulent flow past an airfoil with trailing edge separation', *AIAA J.*, **21**, 1525–1532 (1983).
5. S. Majumdar, 'Role of underrelaxation in momentum interpolation for calculation of flow with nonstaggered grids', *Numer. Heat Trans.*, **13**, 125–132 (1988).
6. T.F. Miller and F.W. Schmidt, 'Use of a pressure-weighted interpolation method for the solution of incompressible Navier–Stokes equations on a non-staggered grid system', *Numer. Heat Trans.*, **14**, 213–233 (1988).
7. D. Lee and J.J. Chiu, 'Covariant velocity-based calculation procedure with nonstaggered grids for computation of pulsatile flows', *Numer. Heat Trans. Part B*, **21**, 269–286 (1992).
8. P. Tamamidis and D.N. Assanis, 'Prediction of three-dimensional steady incompressible flows using body-fitted coordinates', *ASME J. Fluids Eng.*, **115**, 457–462 (1993).
9. M.C. Melaaen, 'Calculation of fluid flows with staggered and nonstaggered curvilinear nonorthogonal grids—the theory', *Numer. Heat Trans. Part B*, **21**, 1–19 (1992).
10. M. Peric, 'Analysis of pressure–velocity coupling on nonorthogonal grids', *Numer. Heat Trans. Part B*, **17**, 63–82 (1990).
11. M.J. Cho and M.K. Chung, 'New treatment of nonorthogonal terms in the pressure correction equation', *Numer. Heat Trans. Part B*, **26**, 133–145 (1994).
12. H. Xu and C. Zhang, 'Study of the effect of the non-orthogonality for non-staggered grids—the results', *Int. j. numer. methods fluids*, submitted.
13. S.V. Patankar and D.B. Spalding, 'A calculation procedure for heat, mass and momentum transfer in three-dimensional parabolic flows', *Int. J. Heat Mass Trans.*, **15**, 1787–1806 (1972).
14. J.P. Van Doormaal and G.D. Raithby, 'Enhancements of the SIMPLE method for predicting incompressible fluid flows', *Numer. Heat Trans.*, **7**, 147–163 (1984).
15. S.V. Patankar, *Numerical Heat Transfer and Fluid Flow*, Hemisphere, Washington, DC, 1980.

